# Phase Behavior of Associating Polyelectrolyte Polysaccharides. 1. Aggregation Process in Dilute Solution

**Catherine Esquenet and Eric Buhler***

*Centre de Recherche sur les Macromolécules Végétales-CNRS, affiliated with Joseph Fourier University, BP53, 38041 Grenoble, Cedex 9, France*

*Received March 14, 2001; Revised Manuscript Received May 9, 2001*

ABSTRACT: We have examined the structure of hydrophobically modified chitosans in a selective aqueous solution at $T = 25$ °C, i.e., a nonsolvent for the alkyl grafted chains and a good solvent for the polyelectrolyte chitosan backbone. The behavior of the hydrophobically modified chitosan was investigated using viscosity and static and dynamic light scattering. We observed three regions on the phase diagram of the associative polymer in aqueous solution: (i) a supernatant phase (unimers phase) at low polymer concentration; (ii) solutions of intermolecularly bridged "flowerlike" micelles at intermediate polymer concentration; (iii) an associative gel phase at high polymer content. The aggregation process in dilute regime was investigated using combined static and dynamic light scattering. In particular, the concentration dependence of the aggregation number, of the micellar aggregates size, of the micelle concentration, and of the unimer concentration is discussed.

## 1. Introduction

Over the past two decades hydrophobically modified water-soluble polymers or so-called associating polymers have found an increasing number of applications. Because of their extraordinarily viscosifying properties, they are used as thickening agents in paints, in cosmetics, for enhanced oil recovery,[1−5] etc. These new materials are water-soluble polymers bearing a small amount of highly hydrophobic groups.[6−8] Also, many studies have been devoted to hydrophobically modified polyelectrolyte polysaccharides, i.e., polysaccharides with low levels of hydrophobic groups (i.e., 1−5%).[9−11]

Hydrophobically associating polyelectrolytes have shown unusual rheological features and high solubilization properties in aqueous media. These properties arise from the inter- or intramolecular interaction among hydrophobic groups, providing hydrophobic microdomains in an isotropic aqueous solution. The self-association of hydrophobic groups covalently linked to water-soluble polymers can occur either within a single polymer chain or among different polymer chains, or both. In highly dilute aqueous solutions, in general, intrapolymer hydrophobe association may be favorable, but with an increase in the polymer concentration, interpolymer hydrophobe association tends to occur. Polyelectrolyte polymers with a low level of hydrophobic groups show a strong tendency for interpolymer associations even at very low polymer concentrations.[12] Polymers with a strong tendency for interpolymer association may lead to a large increase in solution viscosity with an increase in polymer concentration, which may be followed by gelation upon further increasing polymer concentration. In contrast, polymers with a strong propensity for intrapolymer associations may lead to the formation of a polymer micelle made up with a single macromolecular chain ("unimolecular micelle" or "unimermicelle"[13]) independent of polymer concentration, yielding much less viscous aqueous solutions even at very high polymer concentrations. The understanding of hydrophobically modified polyelectrolyte polysaccharides is another important challenge as they are often encountered in many biological systems. Also, hydrophobic associations occur in competition with electrostatic repulsions. However, theoretical works describing the properties of associating polyelectrolytes are practically absent.[14−16]

In the present work, we have examined the structure of hydrophobically modified chitosans (HMC) with a hydrophobic substitution degree of 2%. The HMC consists of alkyl chains grafted to the polyelectrolyte backbone. In acid conditions, chitosan is water-soluble due to the presence of protonated amino groups, and it exhibits a polyelectrolyte character. The length and the number of alkyl chains along the polycationic backbone control the degree of hydrophobicity of HMC. In the present paper, we report the results of the viscosity and light scattering experiments performed on 0.3 M acetic acid/0.05 M sodium acetate solutions of HMC for polymer concentration ranging from $2 \times 10^{-6}$ to $7.5 \times 10^{-3}$ g/cm$^3$. We present also the light scattering study of the aggregation process in dilute regime (regime characterized by dilute micellar aggregates). Also, a partial phase diagram length of the alkyl side chains−polymer concentration has been determined at fixed temperature $T = 25$ °C. The length of the alkyl chains was varying from C6 to C14. Three main domains have been delimited: a supernatant phase, an intermolecularly bridged spherical "flowerlike" micelles domain is proposed, and a gellike domain. The structural properties of the different phases of the phase diagram were investigated by means of static and dynamic light scattering.

In section 2 of the paper we describe materials and experimental techniques used in this study. In section 3 we report the results of the experiments.

## 2. Materials and Methods

**2.1. Sample Characteristics.** We have investigated solutions of the hydrophobically modified polysaccharide chitosans (HMC). Alkyl side chains are grafted to the main chitosan chain, which is a semirigid polyelectrolyte (the intrinsic persistence length of chitosan is roughly equal to 80 Å).[17] Chitosan is a polysaccharide from PROTAN composed of $\beta$ 1→4 D-glucosamine units with a degree of N-acetylation equal to 12%. The polysaccharide chitosan belongs to a family of linear

10.1021/ma010451j CCC: $20.00 
Published on Web 06/19/2001

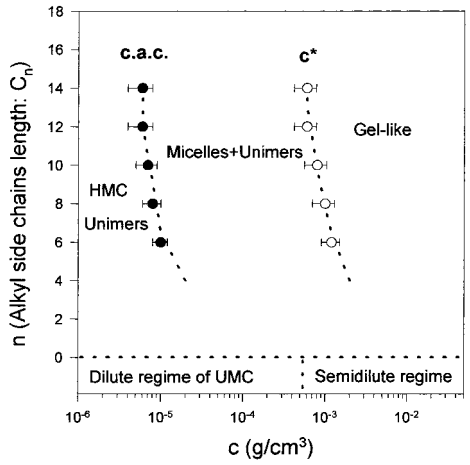


**Figure 1.** Phase diagram in the alkyl side chains length−polymer concentration plane at a fixed temperature $T = 25$ °C. Points (●) represent the unimers−micelles transition (i.e., the critical aggregation concentration deduced from static light scattering measurements), and the points (○) represent micelles−gel transition (i.e., the concentration $c^*$ deduced from viscosity mesurements). The degree of alkylation is equal to 2%. The length of the alkyl side chains is defining by $C_n$, with $n$ varying from 6 to 14. The phase behavior of the analogue unmodified chitosan (i.e., C0) is also represented.

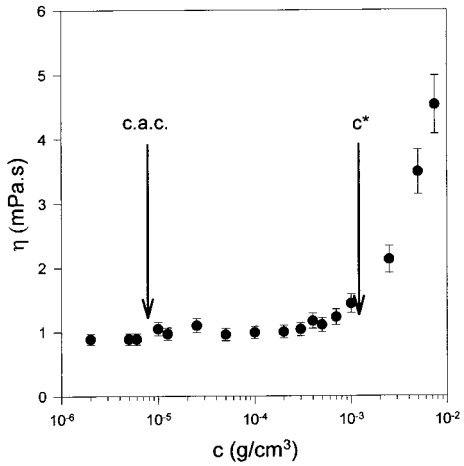


**Figure 2.** Variation of the solution viscosity $\eta$ with the C8 HM-chitosan concentration. Arrows indicate the cac and the concentration $c^*$.

cationic biopolymers obtained from alkaline N-deacetylation of chitin, which is the second most abundant polymer in nature. The mass $M_w = 195\,000 \pm 5000$ g/mol and the polydispersity $M_w/M_n = 1.3$ were determined by GPC and light scattering,[17,18] where $M_w$ is the weight-average molecular weight and $M_n$ the number-average molecular weight. The contour length is equal to $L_c = 6000$ Å. The solutions were investigated in the polymer concentration range from $2 \times 10^{-6}$ to $7.5 \times 10^{-3}$ g/cm$^3$ at 25 °C and in the solvent 0.3 M acetic acid ($CH_3COOH$) in the presence of sodium acetate ($CH_3COONa$). The concentration of sodium acetate (excess of salt) was equal to 0.05 M. For a 0.3 M concentration in acetic acid, all the amino groups are protonated, and chitosan exhibits a polyelectrolyte character.[17,18] This medium is a good solvent for the chitosan main chain and a bad solvent for the alkyl side chains.

The hydrophobically modified samples were prepared by reaction with the amino groups of the backbone of the polymer chain with C6 to C14 aldehyde. The modification procedure employed here is similar to the method described earlier.[19,20] The degree of alkylation used in this work is equal to 2% and has been checked by $^1$H NMR measurements[19] (2% of the monomers are bearing an alkyl chain). The hydrophobically modified chitosans (HMC) are equivalent to their unmodified analogue; the main chitosan chain is the same for all samples investigated. The mass of the HMC sample was then calculated (for example, the mass of the C8 HMC is estimated to be equal to $M_w = 197\,600 \pm 5000$ g/mol). The length of the alkyl side chains was varying from C6 to C14.

To carry out the static and dynamic light scattering experiments, all the solutions were filtered directly into the light scattering cells through 0.2 $\mu$m Sartorius cellulose nitrate membranes. The solutions were filtered also before viscosity and GPC measurements. No aging effects were observed. The solutions were filtered very easily, so insignificant amounts of chitosan derivative may be lost in the filters.

**2.2. Viscosity Measurements.** The viscosity measurements were carried out by using a low-shear 40 coaxial viscometer, on the Newtonian plateau, within the range of polymer concentration from $2 \times 10^{-6}$ to $7.5 \times 10^{-3}$ g/cm$^3$, which is the same as for the light scattering experiments (see Figure 2).

**2.3. Static Light Scattering.** Static light scattering (SLS) and dynamic light scattering (DLS) experiments were performed by means of a spectrometer equipped with an argon ion laser (Spectra Physics model 2020) operating at $\lambda = 488$ nm, an ALV-5000 correlator (ALV, Langen-Germany Instruments), a computer-controlled and stepping-motor-driven variable angle detection system, and a temperature-controlled sample cell. The temperature was $25 \pm 0.1$ °C unless otherwise noted. The scattering spectrum was measured through a band-pass filter (488 nm) and a pinhole (200 $\mu$m for the static experiments and 100 or 50 $\mu$m for the dynamic experiments) with a photomultiplier tube (ALV).

In the SLS experiments, the excess of scattered intensity $I(q)$ was measured with respect to the solvent, where the magnitude of the scattering wave vector $q$ is given by

$$q = \frac{4\pi n}{\lambda} \sin\frac{\theta}{2} \tag{1}$$

In eq 1, $n$ is the refractive index of the solvent (1.34 for the water at 25 °C), $\lambda$ is the wavelength of light in the vacuum, and $\theta$ is the scattering angle. In our experiments, the scattering angle $\theta$ was varied between 20° and 150°, which corresponds to scattering wave vectors $q$ in the range from $6 \times 10^{-4}$ to $3.2 \times 10^{-3}$ Å$^{-1}$. The absolute scattering intensities $I(q)$ (i.e., the excess Rayleigh ratio) were deduced by using a toluene sample reference for which the excess Rayleigh ratio is well-known.

A virial expression for the osmotic pressure can be used in dilute regime to deduce the following relationship:

$$\frac{Kc}{I(q,c)} = \frac{1}{M_w}\left[1 + q^2\frac{R_G^2}{3} + ...\right] + 2A_2Q(q,c)c + ... \tag{2}$$

The function $Q(q,c)$ is approximately unity for flexible polymer chains but not for spheres,[21] and $Q(0,c)$ is equal to 1 in any case. $c$ is the polymer concentration, and $A_2$ is the second virial coefficient, which describes the polymer−solvent interactions. The scattering constant is $K = 4\pi^2n^2(dn/dc)^2/N_A\lambda^4$ where $dn/dc$ is the refractive index increment and $N_A$ is Avogadro's number. The $dn/dc$ of the polysaccharide chitosan in the solvent composed of 0.3 M acetic acid + sodium acetate is equal to 0.195.[18] The plots of $c/I(q,c)$ vs $q^2$ were extrapolated to $q = 0$ to give intercepts $c/I(0,c)$. If the length scale $q^{-1}$ is sufficiently large compared to the radius of gyration $R_G$ of the polymers, the form factor obeys Guinier's law and the apparent radius of gyration $R_{G,app}$ can be determined from the intercept and the initial slope of these plots using a scattering inverse Lorentzian law of the form[21]

$$\frac{c}{I(q,c)} = \frac{c}{I(0,c)}\left[1 + \frac{q^2R_{G,app}^2}{3}\right] \quad \text{if } qR_G \ll 1 \tag{3}$$

The weight-average molecular weight[21] $M_w$ can be obtained from

$$\frac{I(0,c)}{Kc} = M_{w,app} = M_w(1 - 2A_2M_wc) \quad (4)$$

The apparent mass $M_{w,app}$ of polymers in solution at a concentration $c$ is given by extrapolation of the scattered intensity $I(q)/c$ to $q = 0$, while the apparent radius of gyration is obtained by a mean-square linear fit of the inverse of the scattered intensity vs $q^2$.

**2.4. Dynamic Light Scattering.** In the dynamic light scattering experiments (DLS), the normalized time autocorrelation function $g^{(2)}(q,t)$ of the scattered intensity is measured.[21]

$$g^{(2)}(q,t) = \frac{\langle I(q,0)\, I(q,t)\rangle}{\langle I(q,0)\rangle^2} \quad (5)$$

The latter can be expressed in terms of the field autocorrelation function or equivalently in terms of the autocorrelation function of the concentration fluctuations $g^{(1)}(q,t)$ through

$$g^{(2)}(q,t) = A + \beta|g^{(1)}(q,t)|^2 \quad (6)$$

where $A$ is the baseline and $\beta$ is the coherence factor which in our experiments is equal to 0.7−0.9. The normalized dynamical correlation function $g^{(1)}(q,t)$ of polymer concentration fluctuations is defined as

$$g^{(1)}(q,t) = \frac{\langle \delta c(q,0)\, \delta c(q,t)\rangle}{\langle \delta c(q,0)^2\rangle} \quad (7)$$

where $\delta c(q,t)$ and $\delta c(q,0)$ represent fluctuations of polymer concentration at time $t$ and zero, respectively.

In our experiments, the inspection of the angular dependence shows that the relaxations are diffusive with characteristic time inversely proportioned to $q^2$. Some of our solutions were characterized by a single relaxation mechanism ($c <$ critical aggregation concentration). For these solutions we have adopted the classical cumulant analysis.[22] This analysis provides the variance of the correlation function and the first reduced cumulant $(\tau q^2)^{-1}$ where $\tau$ is the average relaxation time of $g^{(1)}(q,t)$. The extrapolation of $(\tau q^2)^{-1}$ to $q = 0$ yields the values of the mutual diffusion constant $D$. The latter is related to the average hydrodynamic radius $R_H$ of the macromolecules and of the micelles through

$$D = \frac{kT}{6\pi\eta_s R_H} = \left(\frac{1}{\tau q^2}\right)_{q^2=0} \quad (8)$$

where $k$ is the Boltzmann constant, $\eta_s$ the solvent viscosity, and $T$ the absolute temperature.

We also used another method to determine the average relaxation time $\tau$: the Contin method based on the inverse Laplace transform of $g^{(1)}(q,t)$.[23] If the spectral profile of the scattered light can be described by a multi-Lorentzian curve, then $g^{(1)}(q,t)$ can be written as

$$g^{(1)}(q,t) = \int_0^\infty G(\Gamma)\exp(-\Gamma t)\, d\Gamma \quad (9)$$

where $G(\Gamma)$ is the normalized decay constant distribution. This method is more appropriate for the solutions characterized by several relaxations mechanisms (e.g., mixture of micelles and unimers).

## 3. Results and Discussion

**3.1. Partial Phase Diagram of HMC.** Figure 1 shows the phase diagram in the polymer concentration−alkyl side chain length plane at fixed temperature $T =$ 25 °C and at fixed degree of alkylation 2%. The solvent is a 0.3 M acetic acid + 0.05 M sodium acetate aqueous solution. The excess salt concentration being large, the charges of the polyelectrolyte main chain may be screened. The partial phase diagram of the HMC was obtained by visual inspection, by viscosity and light scattering experiments for polymer concentration varying from 0 to $10^{-2}$ g/cm$^3$ and for alkyl side chain length varying from C6 to C14. In Figure 1 is also represented the phase behavior of the unmodified chitosan (UMC) characterized by an alkyl side chain length equal to zero, i.e., C0. The phase behavior of the UMC in solution shows the classical sequence: dilute regime, semidilute regime.[17]

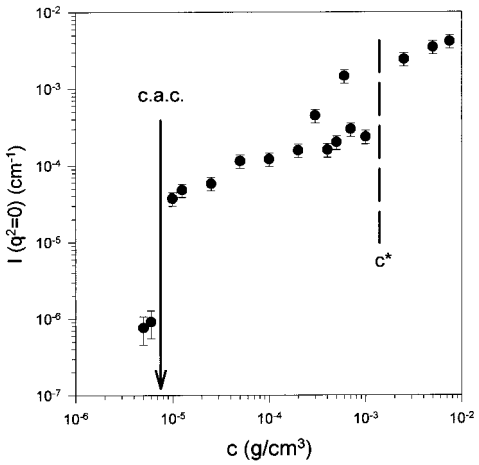


**Figure 3.** Light scattering intensity at zero angle as a function of the C8 HMC concentration $c$. Above the critical aggregation concentration, cac, the intensity increases strongly with the polymer concentration. The arrow indicates the cac, and the vertical dashed line represents the transition between micelles and gel regime.

Upon increasing associating polysaccharide content (HMC), we have identified three regions on the phase diagram: (i) a supernatant phase (isolated HMC polymer chains), (ii) a micellar phase, and (iii) an associative gel phase. At low polymer concentrations (i.e., at concentrations below the critical aggregation concentration cac), the supernatant phase corresponds to free isolated HMC polymer chains dissolved in the solvent, which will be called unimers in what follows. Intermediate HMC contents (cac $< c < c^*$) correspond to a micellar aggregates (associations of unimers) phase that does not exhibit an increase of the solution viscosity (see Figure 2). These micelles are then not connected and are diluted in the solvent. The structure of these aggregates will be described in part 3.4. At higher polymer concentrations ($c > c^*$), the system exhibits a large increase of the solution viscosity and a gellike behavior (see Figure 2). The points corresponding to micelles−gel transitions ($c = c^*$) were deduced from the viscosity measurements and from visual inspection. Figure 2 shows the polymer concentration dependence of the solution viscosity $\eta$ for a HMC sample characterized by C8 alkyl side chains. The arrows indicate the cac and the $c^*$ concentration. The critical aggregation concentration (cac) was determined by static light scattering. For a concentration smaller than the cac the molecular weight measured by light scattering corresponds to the mass of a free polymer. For concentrations larger than the cac, the molecular weight and then the scattered intensity extrapolated to zero wave vector, $I(0)$, are much larger and correspond to micellar aggregates. No excess scattering at low angles (20°−30°) was observed in this regime.

In Figure 3, the measured light scattered intensity extrapolated to zero wave vector, $I(q^2=0)$, is plotted as

a function of the polymer concentration $c$ for the HMC C8 sample. At a concentration below the critical aggregation concentration, cac = $(8 \pm 2) \times 10^{-6}$ g/cm$^3$, the scattered intensity increases slowly with the concentration, which indicates an increase of the unimers concentration. Extrapolation to zero wave vector of light scattering intensity measurements in this concentration range allows us to determine the apparent weight-average molecular weight of the C8 HM-chitosan polymer chain: $M_{w,app} \sim 197\,600$ g/mol. The low level of the scattered intensity in this concentration range leads to an approximate determination of the value of the unimer molecular weight (error ~ 40%). At concentration above cac, the scattered intensity increases strongly with the concentration, and this is interpreted as being due to the growth process of associating polyelectrolyte aggregates. The scattered intensity is still increasing for polymer concentrations larger than $c^*$. In this regime the scattered intensity should decrease with increasing concentration due to the screening of concentration fluctuations, as expected for semidilute solutions.[24,25] The cac is smaller for the C6 HMC sample. This phase diagram is similar to the theoretical phase diagram proposed by Vasilevskaya et al. for associating polyelectrolytes.[14]

**3.2. Dynamic Light Scattering.** In the following parts of the paper we present the light scattering experiments performed on aqueous solutions of C8 HM-chitosan.

**3.2.1. Concentration Range: $c$ < cac.** In the present study $g^{(1)}(q,t)$ was measured below and above the critical aggregation concentration. In the concentration range below the cac, $g^{(1)}(q,t)$ is found to be a simple exponential decay in the entire $q$ range. The diffusion coefficient $D$ is found to be independent of the scattering wave vector $q$ and is found to be equal to

$$D = \left(\frac{1}{\tau q^2}\right)_{q^2 \to 0} = (1.75 \pm 0.40) \times 10^7 \quad \text{nm}^2/\text{s} \qquad (10)$$

leading to the hydrodynamic radius:

$$R_H = 14 \pm 3 \quad \text{nm} \qquad (11)$$

This result is consistent with the diffusive motion of isolated polymer chains (unimers) which are present in the solution (supernatant phase). The low level of the scattered intensity in this concentration range leads to a large error bar for $R_{H,unimers}$ (even for 200 $\mu$m pinhole). Also, the radius of gyration of unimers is too small to be measured by static light scattering. It is then not possible to discuss the ratio $R_H/R_G$ for unimers. In this regime spherical "flowerlike unimermicelles" are expected.[13,16,26]

However, light scattering experiments were performed under the unmodified analogue 195 000 chitosan chain.[17,18] The solvent was also a 0.3 M $CH_3COOH$ + 0.05 M $CH_3COONa$ solution, and the temperature was also equal to $T = 25$ °C. For the radius of gyration and the hydrodynamic radius, we found $R_G = 70 \pm 10$ nm and $R_H = 48 \pm 4$ nm, respectively. The positive sign of the second virial coefficient, $A_2 = (4.47 \pm 0.50) \times 10^{-3}$ cm$^3$ g$^{-2}$ mol, indicates that at these conditions the 0.3 M $CH_3COOH$ + 0.05 M $CH_3COONa$ medium is a good solvent for the unmodified chitosan. The large difference between the hydrodynamic radius of the free HM-chitosan chain and of the unmodified analogue chitosan chain is related to the intrapolymer hydrophobic associations which may lead to the formation of a polymer micelle made up with a single C8 HMC macromolecular chain ("unimermicelle").

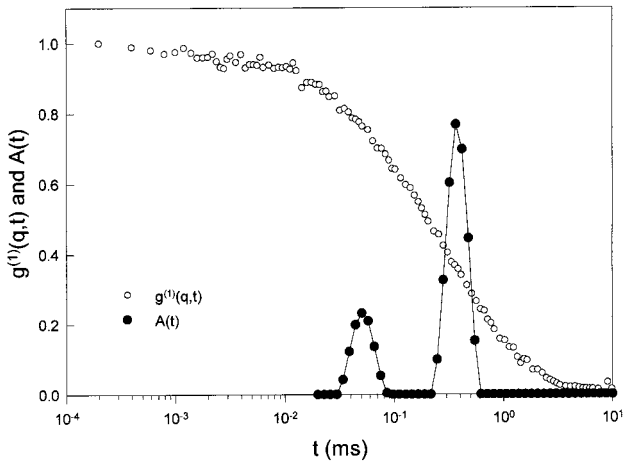


**Figure 4.** Semilog representation of $g^{(1)}(q,t)$ for $\theta = 120°$ relative to a C8 HMC solution at polymer concentration $c = 4 \times 10^{-4}$ g/cm$^3$ (○). The distribution function of decay times $A(t)$ obtained using the Contin method is also represented (●).

**3.2.2. Concentration Range: cac < $c$ < $c^*$.** In the concentration range above the cac, the time autocorrelation function of the scattered electric field can be described by a sum of two relaxations widely separated in time. Figure 4 shows the semilog plot of $g^{(1)}(q,t)$ for a C8 HM-chitosan solution at a polymer concentration equal to $4 \times 10^{-4}$ g/cm$^3$, i.e., for a concentration larger than the critical aggregation concentration. The scattering angle $\theta$ is equal to 120°.

$$g^{(1)}(q,t) = \frac{\langle E^*_{fast}(q,0)\, E_{fast}(q,t)\rangle + \langle E^*_{slow}(q,0)\, E_{slow}(q,t)\rangle}{\langle I(q)\rangle}$$

$$g^{(1)}(q,t) = A_{fast}(q) \exp\left(\frac{-t}{\tau_{fast}}\right) + A_{slow}(q) \exp\left(\frac{-t}{\tau_{slow}}\right) \qquad (12)$$

$E_{fast}(q)$ and $E_{slow}(q)$ are respectively the fast and the slow electric scattered field and are fluctuating independently. $\tau_{fast}$ and $\tau_{slow}$ are respectively the fast and the slow relaxation time. $A_{fast}(q)$ and $A_{slow}(q)$ are the corresponding amplitudes. Figure 4 also shows a typical example of results obtained by applying the Contin method to our data. $A(t)$ is the normalized distribution function of decay times obtained by using the Contin method. We clearly distinguish slow and fast modes well separated in time. In this regime, one expects for the time relaxation function $g^{(1)}(q,t)$ (a) a fast relaxation time corresponding to the diffusive mode of unimers and (b) a slow relaxation time corresponding to the diffusion of the micellar aggregates.

The inspection of Figure 5, representing the variation of the products $1/\tau_{fast}q^2$ and $1/\tau_{slow}q^2$ with $q^2$ for a polymer solution at a concentration equal to $4 \times 10^{-4}$ g/cm$^3$, shows clearly that the fast and the slow mode are diffusive modes with characteristic times $\tau_{fast}$ and $\tau_{slow}$ inversely proportioned to $q^2$. Thus, it is possible to calculate for each polymer concentration a fast diffusion coefficient $D_{fast}$ and a slow diffusion coefficient $D_{slow}$ using eq 8. Experimentally, one obtains a diffusion coefficient $D_{fast} = 1/\tau_{fast}q^2$ independent of the scattering wave vector and of the concentration, which is equal to

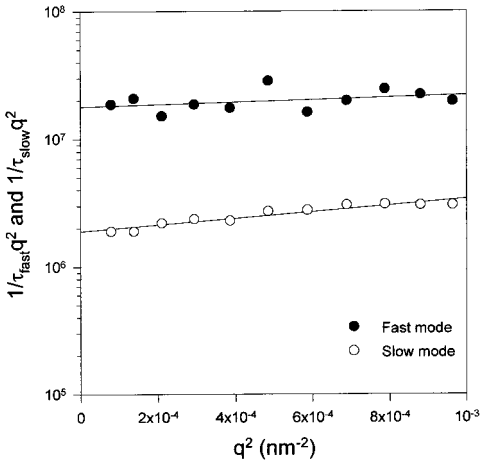


**Figure 5.** Variation of $1/\tau_{fast}q^2$ (●) and of $1/\tau_{slow}q^2$ (○) with $q^2$ measured in a C8 HMC solution at a polymer concentration $c = 4 \times 10^{-4}$ g/cm$^3$. Black lines represent linear least-squares best fits.

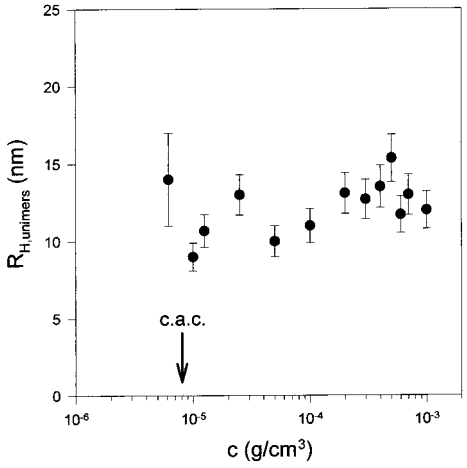


**Figure 6.** Dependence of the hydrodynamic radius of the unimers on the total C8 HMC concentration, deduced from the fast time mode of the quasi-elastic light scattering relaxation function. The arrow indicates the cac.

the diffusion coefficient measured below the cac. This confirms the previous interpretation, which assigned the fast relaxation time to the diffusive motion of unimers. Figure 6 shows the independence of the hydrodynamic radius of the unimers on the polymer concentration.

$$R_{H,unimers} = \frac{kT}{6\pi\eta_s D_{fast}(q^2 \rightarrow 0)} \qquad (13)$$

Apparently, there is a weak concentration dependence. The hydrodynamic radius of the micelles $R_{H,micelles}$ over the polymer concentration range of $1 \times 10^{-5}$–$1 \times 10^{-3}$ g/cm$^3$ at $T = 25$ °C is presented in Figure 7.

$$R_{H,micelles} = \frac{kT}{6\pi\eta_s D_{slow}(q^2 \rightarrow 0)} \qquad (14)$$

Data reveal an increase of the micelles hydrodynamic radius with increasing polymer content in the whole polymer concentration range. $R_{H,micelles}$ reach values around 160 nm for $c > 10^{-4}$ g/cm$^3$. We will discuss values of $R_{H,micelles}$ in the part 3.4.

**3.3. Aggregation Process in Dilute Regime (cac < *c* < *c**).** Another interesting discussion can be made by examination of the behavior of the relative amplitudes $A_{fast}$ and $A_{slow}$. The sum of the amplitudes is equal to 1.

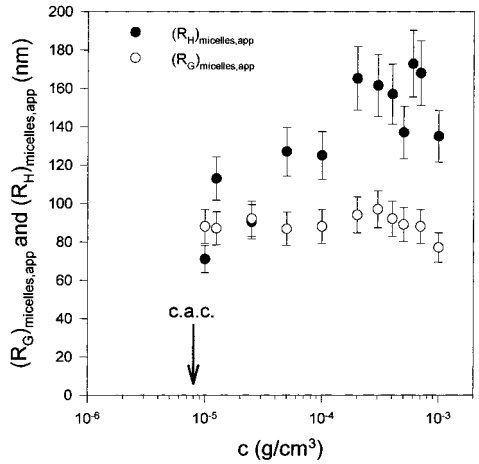


**Figure 7.** Variation of the apparent hydrodynamic radius of the micelles $(R_H)_{micelles,app}$ (●) and of the apparent radius of gyration of the micelles $(R_G)_{micelles,app}$ (○) with the C8 HMC concentration in the polymer concentration range cac < *c* < *c**.

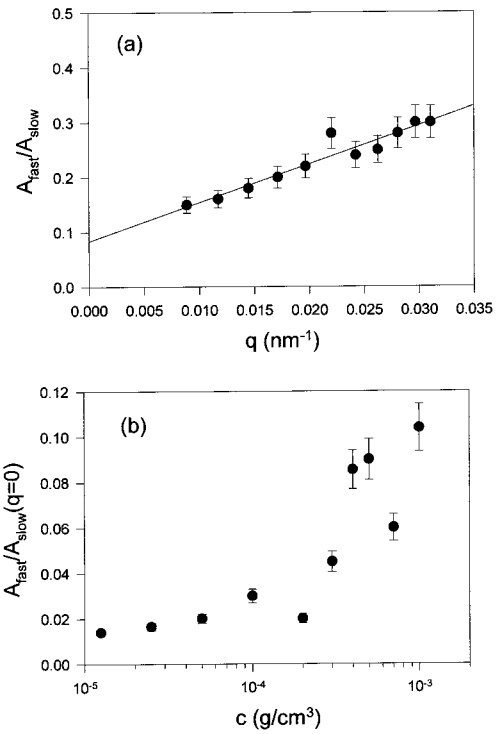


**Figure 8.** Scattering wave vector dependence (a) of $A_{fast}/A_{slow}$ for a $c = 4 \times 10^{-4}$ g/cm$^3$ C8 HMC solution and polymer concentration dependence (b) of $A_{fast}/A_{slow}(q=0)$. The black line represents the fit of the data.

$$A_{fast}(q) + A_{slow}(q) = 1 \qquad (15)$$

It is worth noting that in fact these amplitudes are dependent on the scattering wave vector $q$, as shown in Figure 8. Figure 8a shows the $q$ dependence of the ratio $A_{fast}/A_{slow}$ for a C8 HMC solution at a concentration $c = 4 \times 10^{-4}$ g/cm$^3$ and at temperature $T = 25$ °C. The increase of $A_{slow}$ with the decrease of $q$ confirms that the slow mode is due to aggregates. The variation of $A_{fast}/A_{slow}$ extrapolated to zero wave vector with the total polymer concentration can be observed in Figure 8b. This concentration dependence and the scattered in-

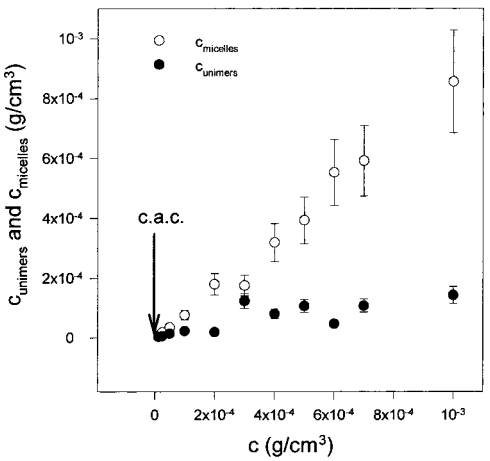


**Figure 9.** Variation of unimer (●) and micelle (○) concentrations vs the total C8 HMC concentration *c*. The arrow indicates the cac.

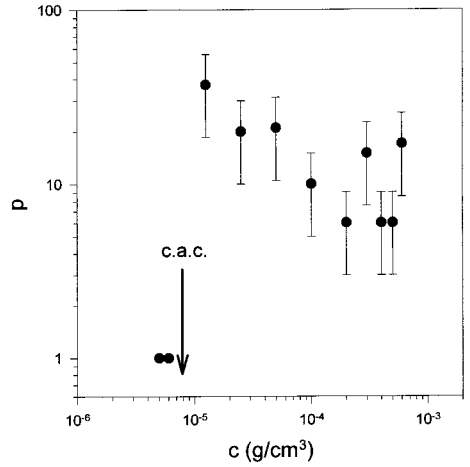


**Figure 10.** Variation of the aggregation number *p* as a function of the C8 HMC concentration. Below the cac *p* is equal to 1 (unimers phase). The arrow indicates the cac.

tensity $I(q)$ can provide more information about the aggregation process. The amplitudes measured by dynamic light scattering can be used to analyze the static light scattering results.[18,27,28] Defining $I_{unimers}(q)$ and $I_{micelles}(q)$ as the time-average intensities associated with the fluctuations of polymer concentration with respectively short and long relaxation times and using the normalization condition

$$g^{(1)}(q,0) = A_{fast}(q) + A_{slow}(q) = 1 \qquad (16)$$

we obtain

$$I_{unimers}(q) = A_{fast}(q)\, I(q)$$
$$I_{micelles}(q) = A_{slow}(q)\, I(q) \qquad (17)$$

The value of the total intensity $I(q)$ was deduced directly from the static light scattering measurements.

$$I(q) = I_{unimers}(q) + I_{micelles}(q) \qquad (18)$$

To evaluate the concentration of unimers and the concentration of micelles as a function of the total concentration, we applied the following procedure: Let the molecular weight of free polymer chains and micelles be $M_{unimers}$ and $M_{micelles} = pM_{unimers}$ (where $p$ is the aggregation number, i.e., the number of unimers constituting a micelle and $M_{unimers} = 197\,600$ g/mol). The corresponding concentrations of free unimers and unimers in micelles are $c_{unimers}$ and $c_{micelles}$, respectively. The total concentration of the solution $c$ is equal to the sum of the concentrations.

$$c = c_{unimers} + c_{micelles} \qquad (19)$$

From the scattered intensity of unimers $I_{unimers}$ and neglecting interactions between unimers and/or micelles, we deduced the concentration of unimers:

$$c_{unimers} = \frac{I_{unimers}(q\rightarrow 0)}{KM_{unimers}} = \frac{A_{fast}(q\rightarrow 0)\, I(q\rightarrow 0)}{KM_{unimers}} \qquad (20)$$

where $K$ is the scattering constant (see eq 2). From the concentration of unimers $c_{unimers}$ and the total concentration $c$, we calculate the concentration of the polymer in micelles $c_{micelles} = c - c_{unimers}$ (see eq 19). Figure 9 shows the variation of the concentration of unimers, $c_{unimers}$, and of the micelles, $c_{micelles}$, as a function of the total polymer concentration $c$. The polymer is a C8 HMC sample. The unimer concentration is expected to saturate and to be equal to the critical aggregation concentration (cac). A continuous increase of $c_{unimers}$ and $c_{micelles}$ with the total polymer concentration is found. This result is in opposition to the classical micellization picture within which the degree of association $p$ and the concentration of unimers are expected to be independent of the concentration (the concentration of unimers is expected to be equal to the cac).[29,30] Such a nonconstant unimer concentration would imply a polydisperse population of unimers and aggregates.

The concentration dependence of the aggregation number $p$ at $T = 25$ °C deduced using this analysis is presented in Figure 10 for the C8 HM-chitosan sample. In doing so, the effect of the second virial coefficient between micelles is neglected.

$$p = \frac{M_{micelles}}{M_{unimers}} = \frac{I_{micelles}(q\rightarrow 0)}{Kc_{micelles}M_{unimers}} = \left(\frac{A_{slow}}{A_{fast}}\right)_{q\rightarrow 0}\frac{c_{unimers}}{c_{micelles}} \qquad (21)$$

According to the classical micellization model,[29,30] the aggregation number $p$ is expected to be independent of the polymer concentration. In the present study, the error bar of the aggregation number being large, it is difficult to say whether the curve exhibits a slight decrease of the aggregation number with the concentration. However, data reveal aggregation number $p$ values of ∼15−20 over the whole polymer concentration range. Above the cac associating polyelectrolytes associate in polydisperse aggregates with a small association number ($p \sim 15-20$) and large hydrodynamic radius (up to 160 nm). Similar experimental results were already observed for polydisperse and loose triblock copolymer aggregates.[27,31] Also, note that identical values for the association number are often observed with associating polymers.[32]

**3.4. Structure of the Micelles (cac < *c* < *c**).** The slow mode was interpreted as caused by the formation of micelles. Figure 7 shows the variation of the apparent hydrodynamic radius and of the apparent radius of gyration of the micelles in the dilute regime (regime where the solution viscosity is constant). The apparent radius of gyration of the micelles $(R_G)_{micelles,app}$ was determined using the following relation:

$$I_{micelles}(q,c_{micelles}) = I_{micelles}(0,c_{micelles}) \times \left[1 - \frac{1}{3}q^2(R_G^2)_{micelles,app}\right] \quad \text{if } q(R_G)_{micelles,app} \ll 1 \quad (22)$$

where $I_{micelles}(0,c_{micelles})$ is the slow scattered intensity extrapolated to zero wave vector and $(R_G)_{micelles,app}$ is an apparent radius of gyration for the micelles. Data reveal $(R_G)_{micelles,app}$ values of 90 ± 10 nm over the whole concentration range. Actually, the apparent radius of gyration might approximate the real one because the factor $2A_2M_{w,micelles}c_{micelles}$ is much smaller than 1. The scattered intensity being very low in the concentration range below the cac, it was not possible to evaluate the second virial coefficient between unimers. The relationship between apparent and true mean-square radius of gyration is given by

$$(R_G^2)_{micelles,app} = \frac{3\partial\left[\frac{I_{micelles}(0,c_{micelles})}{I_{micelles}(q,c_{micelles})}\right]}{\partial q^2} = \frac{(R_G^2)_{micelles}}{1 + 2A_2M_{w,micelles}c_{micelles}} \quad (23)$$

Another way to determine the micellar aggregates structure is to consider the ratio $(R_H/R_G)_{micelles}$.[33−35] This ratio is found to be larger than the value of $(5/3)^{1/2} = 1.29$ expected for dense spheres and measured on starlike polymers.[36] A possible micellar structure explaining the value of 1.65 ± 0.25 for the ratio $(R_H/R_G)_{micelles}$ in the concentration range $5 \times 10^{-5}$−$1 \times 10^{-3}$ g/cm$^3$ is the spherical "flowerlike" structure with a dense hydrophobic core and a swollen corona composed of chitosan polyelectrolyte chains. Each micelle, composed of roughly $p = 20$ polymer chains, i.e., composed of roughly 500 hydrophobic grafts, has a radius of gyration of about 90 nm. For the single "flowerlike" micelle, the radius of gyration should tend to the radius of the dense hydrophobic core.[37] It is then possible to evaluate the number of C8 alkyl grafts constituting the core of a single flower micelle using the ratio $^4/_3\pi R_G^3/1.2^3$ = (volume of the core)/(volume of a graft), where 1.2 nm is roughly the length of a C8 alkyl side chain. The value of this ratio (>$10^6$) being much larger than 500, we can conclude that the micellar aggregates cannot be viewed as single "flowerlike micelles" composed of roughly $p = 20$ polymer chains.

The results presented led us to propose a model for the interpolymer aggregates formed by the HM-chitosan in aqueous solution. The alkyl side chains associate both intra- and intermolecularly. Intrapolymer associations lead to a spherical "flower-type" micelle[16,26,32] in which a hydrophobic microdomain formed from alkyl associations is surrounded by loops of chitosan segments. The concurrent interpolymer alkyl associations will link the "flower-type" micelles together, and thus intermolecularly bridged "flower-type" micelles may be formed. Previous experimental and theoretical studies on polyelectrolytes carrying small amounts of hydrophobic pendants have already shown the formation of intermolecularly bridged "flower-type" micelles in dilute aqueous solutions.[12,16,26,38] Yusa et al.[38] have studied polyelectrolytes carrying cholesterol pendants using turbidity, $^1$H NMR, fluorescence, light scattering, and viscosity. On the basis of the characterization data, an intermolecularly bridged "flower-type" micelle model was proposed for the aggregates. Of course, in the present study, further experiments need to be performed to determine the micellar structure. X-ray experiments are scheduled to determine and to study the structure of the micellar aggregates.

Also, data reveal an increase of $R_{H,micelles}$ with polymer content in the low concentration range (cac < $c$ < 5 × $10^{-5}$ g/cm$^3$) (see Figure 7). This can be interpreted by a swelling of the loops of the micelles ($p \sim 15$−$20$) due to the increase of the hydrophobic interpolymer interactions. The radius of gyration of the micelles corresponding roughly to the average distance between the center and the hydrophobic cores constituing a micelle is constant with the polymer concentration.

## 4. Conclusion

In this work, we have examined the structure of hydrophobically modified chitosans (HMC) in aqueous solution. We have identified three regions of the phase diagram (Figure 1) in the length of the alkyl side chains−polymer concentration plane at the fixed temperature $T$ = 25 °C: (i) unimers (isolated polymer chains); (ii) micelles at intermediate polymer concentration; (iii) gel at high polymer content. In this paper, we have reported combined static and dynamic light scattering experiments performed on HM-chitosans in dilute solution (cac < $c$ < $c$*).

The aggregation process is discussed. In particular, unimers were found to coexist with the interpolymer micellar aggregates in polymer concentration range cac < $c$ < $c$*. The HMC polymer chains form multipolymer aggregates, which can be viewed as an assembly of spherical "flowerlike" micelles where polymer chains are "cross-linked" through alkyl associations. X-ray experiments are scheduled to study the structure of the micellar aggregates.

In particular, the unimer concentration depends on the total polymer concentration, whereas the aggregation number looks to be constant over the whole dilute micellar regime. Such a nonconstant unimer concentration would imply a polydisperse population of unimers. Also, light scattering and rheology experiments concerning the gel phase will be presented in a forthcoming paper.

**Acknowledgment.** The authors gratefully acknowledge M. Rinaudo, J. Desbrières, and O. Guetta for the synthesis of the HM-chitosans. It is a pleasure to acknowledge helpful discussions with A. Khokhlov.

## References and Notes

(1) *Principles of Polymer Science and Technology in Cosmetics and Personal Care*; Goddard, E. D., Gruber, J. V., Eds.; Marcel Dekker: New York, 1999.
(2) McCormick, C. L.; Bock, J.; Schults, D. N. In *Encyclopedia of Polymer Science and Engineering;* John Wiley: New York, 1989; Vol. 17, p 730.
(3) Bock, J.; Varadaraj, R.; Schultz, D. N.; Maurer, J. J. In *Macromolecular Complexes in Chemistry and Biology*; Dubin, P. L., Bock, J., Davies, R. M., Schultz, D. N., Thies, C., Eds.; Springer-Verlag: Berlin, 1994; p 33.
(4) *Polymers as Rheology Modifiers*; Schultz, D. N., Glass, J. E., Eds.; Advances in Chemistry Series 462; American Chemical Society: Washington, DC, 1991.
(5) *Hydropilic Polymer, Performance with Environmental Acceptability*; Glass, J. E., Eds.; Advances in Chemistry Series 248; American Chemical Society: Washington, DC, 1996.
(6) Petit, F.; Iliopoulos, I.; Audebert, R.; Szönyi, S. *Langmuir* **1997**, *13*, 4229−4233.
(7) Tanaka, R.; Meadows, J.; Williams, P. A.; Phillips, G. O. *Macromolecules* **1992**, *25*, 1304.

(8) Biggs, S.; Hill, A.; Selb, J.; Candau, F. *J. Chem. Phys.* **1992**, *96*, 1505.
(9) Lee, K. Y.; Jo, W. H.; Kwon, I. C.; Kim, Y. H.; Jeong, S. Y. *Langmuir* **1998**, *14*, 2329−2332.
(10) Kjøniksen, A. L.; Iversen, C.; Nyström, B.; Nakken, T.; Palmgren, O. *Macromolecules* **1998**, *31*, 8142−8148.
(11) Kjøniksen, A. L.; Nyström, B.; Iversen, C.; Nakken, T.; Palmgren, O.; Tande, T. *Langmuir* **1997**, *13*, 4948−4952.
(12) Yusa, S. I.; Hashidzume, A.; Morishima, Y. *Langmuir* **1999**, *15*, 8826−8831.
(13) Yamamoto, H.; Morishima, Y. *Macromolecules* **1999**, *32*, 7469−7475.
(14) Vasilevskaya, V. V.; Potemkin, I. I.; Khokhlov, A. R. *Langmuir* **1999**, *15*, 7918−7924.
(15) Dobrynin, A. V.; Rubinstein, M. *Macromolecules* **1999**, *32*, 915−922.
(16) Dobrynin, A. V.; Rubinstein, M. *Macromolecules* **2000**, *33*, 8097−8105.
(17) Buhler, E.; Guetta, O.; Rinaudo, M. *Int. J. Polym. Anal. Charact.* **2000**, *6*, 155−175.
(18) Buhler, E.; Rinaudo, M. *Macromolecules* **2000**, *33*, 2098−2106.
(19) Desbrières, J.; Rinaudo, M.; Chtcheglova, L. *Macromol. Symp.* **1997**, *113*, 135−149.
(20) Yalpani, M.; Hall, L. D. *Macromolecules* **1984**, *17*, 272−281.
(21) *Photon Correlation and Light Beating Spectroscopy*; Cummins, H. Z., Pike, E. R., Eds.; Plenum Press: New York, 1974.
(22) Koppel, D. E. *J. Chem. Phys.* **1972**, *57*, 4814.
(23) Provencher, S. W. *Makromol. Chem.* **1985**, *82*, 632.
(24) *Scaling Concepts in Polymer Physics*; de Gennes, P. G., Ed.; Cornell University Press: Ithaca, NY, 1979.
(25) Raspaud, E.; Lairez, D.; Adam, M.; Carton, J. P. *Macromolecules* **1996**, *29*, 1269−1277.
(26) Halperin, A. *Macromolecules* **1991**, *24*, 1418−1419.
(27) Raspaud, E.; Lairez, D.; Adam, M.; Carton, J. P. *Macromolecules* **1994**, *27*, 2956−2964.
(28) Buhler, E.; Dobrynin, A. V.; DeSimone, J. M.; Rubinstein, M. *Macromolecules* **1998**, *31*, 7347−7355.
(29) Tuzar, Z.; Kratochvil, P. *Surf. Colloid Sci.* **1992**, *15*, 1.
(30) Halperin, A.; Tirrel, M.; Lodge, T. P. *Adv. Polym. Sci.* **1991**, 100.
(31) Lairez, D.; Adam, M.; Carton, J. P.; Raspaud, E. *Macromolecules* **1997**, *30*, 6798−6809.
(32) Semenov, A. N.; Joanny, J. F.; Khokhlov, A. R. *Macromolecules* **1995**, *28*, 1066−1075.
(33) Schmidt, M.; Nerger, D.; Burchard, W. *Polymer* **1979**, *20*, 582−588.
(34) Burchard, W.; Schmidt, M.; Stockmayer, W. H. *Macromolecules* **1980**, *13*, 580−587.
(35) Burchard, W.; Schmidt, M.; Stockmayer, W. H. *Macromolecules* **1980**, *13*, 1265−1272.
(36) Roovers, J.; Zhou, L. L.; Toporoeski, P. M.; van der Zwan, M.; Iatrou, H.; Hadjichristidis, N. *Macromolecules* **1993**, *26*, 4324.
(37) Yamakawa, H. *Helical Wormlike Chains in Polymer Solutions*; Springer-Verlag: Berlin, 1997.
(38) Yusa, S. I.; Kamachi, M.; Morishima, Y. *Langmuir* **1998**, *14*, 6059−6067.

MA010451J